PHYSICAL REVIEW B, VOLUME 63, 241402(R)

Modeling of molecular hydrogen and lithium adsorption on single-wall carbon nanotubes

Pierre Dubot and Pierre Cenedese
GARS-CECM, CNRS, 15 rue G. Urbain, 94407 Vitry sur Seine, France
(Received 13 February 2001; published 4 June 2001)

Adsorption of lithium and hydrogen onto carbon nanotubes has been modeled using a neglect of diatomic differential overlap semiempirical calculation. Our results predict that lithium can be adsorbed on zig-zag nanotubes with a charge transfer, an adsorption energy, and a vibration frequency which depend on the tube radius and whether the adatom approaches the surface from outside (exo-way) or inside (endo-way). Adsorbed lithium allows the anchoring of molecular hydrogen on the carbon nanotube with a binding energy in a chemisorption regime compared to previous experimental and theoretical works which show that H_2 is physisorbed. We also predict that a shift of the hydrogen stretching mode upon adsorption should be observable experimentally by vibrational spectroscopy.

DOI: 10.1103/PhysRevB.63.241402 PACS number(s): 34.50.−s, 36.40.−c, 68.35.−p, 71.20.Tx

Carbon nanotubes have attracted considerable attention this last decade since their discovery by Iijima in 1991 (Ref. 1) due to their unique structure and properties. Compared to other carbon materials, nanotubes show a wide variety of morphologies going from the single-wall nanotubes (SWNT) to multiple-walled species associated in bundles or isolated.[2] This makes nanotubes challenging materials to relate their atomic structure to their physical properties. In particular, some studies predicted that the electronic properties of SWNT's are highly dependent to their helicity, ranging from semiconducting to metallic. Following simple band folding concepts and graphite band structure,[3–6] it is predicted that armchair nanotubes should always be metallic, while for zig-zag nanotubes vanishing gap can be observed when circumference contains N unit cells with N multiple of 3.

As graphite intercalation compounds [GIC's] present huge variations of physical and chemical properties,[7] some studies have naturally been focused on doping nanotubes with electron donor or acceptor atoms.[8–11] Like graphite, nanotubes should present an amphoteric character accepting or giving electrons to the added element. Recent studies about lithium and potassium adsorption have confirmed this tendency by showing an increase in the electronic conductivity of halogen or alkaline doped SWNT's.[12] Rao *et al.*[13] have also reported a shift of the Raman A_{1g} mode when nanotubes were exposed to alkaline atoms. Those observations make clear the electron transfer between SWNT and the adsorbed element resulting from electronic and vibrational properties modifications.

Focussing on molecular hydrogen interaction with nanotubes, theoretical and experimental studies show that H_2 is physisorbed in nanotubes materials with a global adsorption energy less than 0.1 eV.[14–16] As the GIC's are much more reactive than graphite, alkaline-doped nanotubes should be good candidates for hydrogen storage with a low chemisorption energy, avoiding a high pressure and low-temperature physisorption regime for tubes filling. Nevertheless, recent experiments[10,11] concerning hydrogen storage by alkali-doped nanotubes are controversial and the adsorbed hydrogen amounts as well as the adsorption sites are not clearly determined. Theoretical investigations can be useful to get insights into the reaction mechanism and the adsorbed entities.

In this work, an electronic structure calculation has been used to model the adsorption process of lithium and hydrogen on SWNT. We have used a calculation based on a semiempirical Hartree-Fock linear combination of atomic orbitals scheme following a neglect of diatomic differential overlap (NDDO) approximation within AM1(Austin Model) parametrization.[17] This is one of the most sophisticated non-*ab-initio* computation scheme which neglects all the three and four centers exchange and Coulomb integrals in the calculation, while the corresponding monocentric terms are fitted to experimental data like electron affinities or ionization potentials. NDDO is known to give accurate results for carbon and organic compounds[18] both from electronic structure and regio-selectivity in chemical reactions.[19,20] Our code (independently developed in Fortran 90) can hold runs for more than 500 atoms in a sp basis, taking advantage of the sparsity of the density matrix. A geometry optimization is completed by minimizing the total energy following a Broyden Fletcher Goldfarb Shanno algorithm. Considering the atomic parameters, the lithium's valence levels are described within a $(2s^1 2p^0)$ atomic orbital scheme as it can be suggested by electronic structure calculations concerning simple molecules like LiH (Refs. 21 and 22) which show that a hybrid orbital must be taken into account for Li bonding.

We focus our work on zig-zag tubes. A systematic study on the effect of the tube chirality and radius will follow in a detailed paper. All the tubes studied in this work were built with a C-C distance of 0.142 nm and clusters were saturated with hydrogen to avoid dangling orbitals on the tube edges. The tube's length has been chosen in order to be near the converging limit for the band gap (seven hexagonal units along the tube axis). When the adsorption process was simulated, carbon atoms in the vicinity of the ad-atom were allowed to relax.

We present in Fig. 1 the evolution of the calculated band gap versus the tubes radius computed with our code and compare them to Hamada's results.[4] We observe that the NDDO calculation confirms the predicted property of a zero band gap for tubes with a circumference containing N unit cells with N a multiple of 3. The calculated density of state for a zig-zag nanotube is displayed in Fig. 2 and clearly shows that NDDO computation gives a correct description

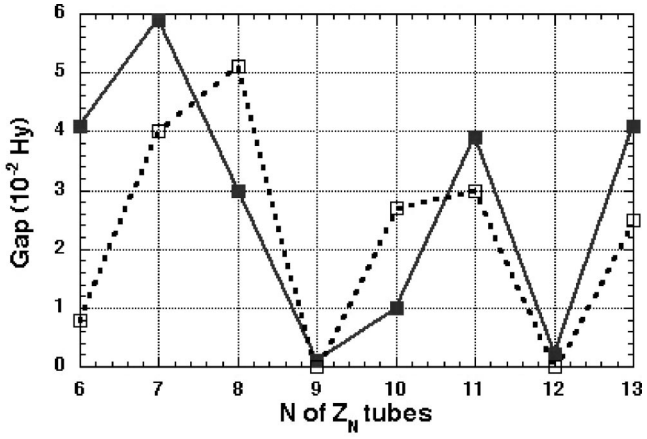

FIG. 1. Gap of zig-zag carbone nanotubes Z_N plotted versus the number N of hexagonal unit cells along the tube circumference. Our results (black squares) are compared to the results of Hamada (Ref. 4).

for the electronic structure of the tube with the lowest unoccupied molecular orbital (LUMO) and the highest occupied molecular orbital (HOMO) energies, respectively, located at -0.160 Hy and -0.190 Hy. The top of the valence band is composed of radial $2p$ states ($2p$ orbitals perpendicular to the tube surface) while levels corresponding to tangential $2p$ orbitals are deeper in energy due to more important orbitals overlapping as it is expected by first order perturbation theory following Eq. (1).

Local charge and molecular orbital spatial distribution are crucial to localize reaction centers and to get insights about the chemical reactivity as the adsorption process and the interaction energy are driven by the frontier orbitals parameters [Eq. (1)] (Ref. 23)

$$E_{int} \approx -2\frac{C_{\mu h}^2 C_{\mu' l'}^2}{\Delta h l'}\,\eta_{\mu\mu'}. \qquad (1)$$

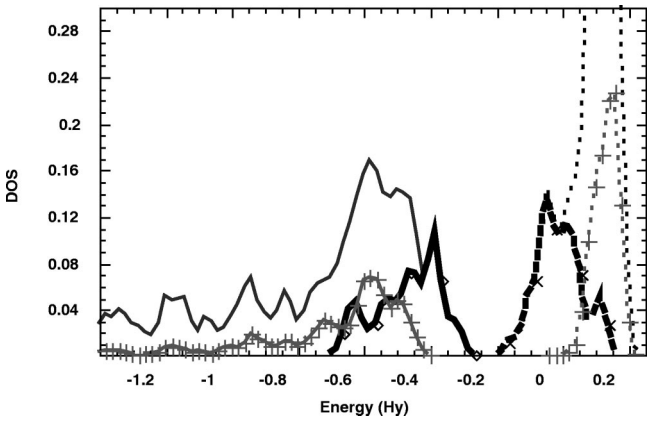

FIG. 2. Local densities of states on a central carbon atom of a Z_8 tube. The radial p-type orbitals (bold) are localized at the top of the valence band (full states) and the bottom of the conduction band (empty states). The tangential p type orbitals (+) are deeper in energy for the full states while at the top of the conduction band for the empty states. The energy reference is the vacuum level.

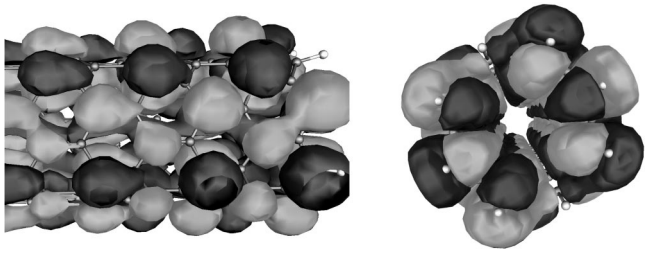

FIG. 3. Face and side views of the Z_8 LUMO lobes constructed on a Gaussian basis set for the atomic orbitals.

In this expression, $\Delta h l' = \mathcal{E}_h - \mathcal{E}_{l'}$ accounts for the energy difference between the HOMO (h) and the LUMO (l') states, $\eta_{\mu\mu'} \approx S_{\mu\mu'}^2$ is proportional to the square of the overlap integral $S_{\mu\mu'}$. $C_{\mu h}$ and $C_{\mu' l'}$ correspond to the components of the HOMO and LUMO eigenstates for the reactants relative to the atomic orbitals localized on the atoms labeled μ and μ'. The Z_8 tube LUMO is displayed in Fig. 3, showing that the lobes are greater outside the tube than inside, driving the overlap orbital and thus the adsorption process. Moreover, we can see that the tube's LUMO phases are antibonding along the tube circumference.

When lithium is adsorbed onto a graphene layer, we found a stable adsorption on top of a hollow site (hexagon's center) at an equilibrium distance of 0.210 nm from the graphene plane. In that case the electron transfer from Li to graphene is 0.72 electron and the adsorption energy -1.70 eV. These results are consistent with what we can expect for GIC's containing alkaline atoms[24] and give good agreement with the work of Hankinson[25] on the cluster model of lithium intercalated graphite using the MP2-RHF (where RHF denotes relativistic Hortree-Fock) calculation. We notice that symmetry of the adsorption site reveals that bonding of lithium involves both its $2s$ and $2p$ orbitals. In fact, if only s type orbital were involved in the interaction, like it is the case of atomic H, the adsorption would arise on top of a carbon atom.[26]

When adsorbed on a zig-zag tube, we found a stable adsorption site outside and inside the tube with Li localized above the center of the nearest tube's hexagon. However, the adsorption energy and the electron transfer depend on the tube radius (Table I) and the side of the lithium approach

TABLE I. Frontier orbitals (HOMO and LUMO) tube's energies in Hartree (H), lithium adsorption energies (eV), and local lithium charge for Li adsorption on Z_N tubes with different radius.

Z_N	HOMO	LUMO	E_{exo}	E_{endo}	$Q_{\text{exo}}^{\text{Li}}$	$Q_{\text{endo}}^{\text{Li}}$
Z_6	-0.181	-0.142	-4.46	-0.82	0.62	0.47
Z_7	-0.207	-0.143	-3.07	-0.63	0.64	0.60
Z_8	-0.190	-0.160	-3.05	-0.70	0.66	0.70
Z_9	-0.176	-0.176	-4.70	-1.93	0.66	0.71
Z_{10}	-0.182	-0.173	-3.56	-1.93	0.68	0.75
Z_{11}	-0.194	-0.161	-5.47	-0.15	0.68	0.77
Z_{12}	-0.179	-0.179	-3.45	-3.90	0.68	0.77
Z_{13}	-0.203	-0.160	-2.40	-1.14	0.69	0.77

(endo-way or exo-way). The results in Table I show that the electron transfer is a smooth varying function of the tube radius and is always greater when lithium is adsorbed inside the tube. A detailed analysis of the adsorbed lithium orbital populations reveals 0.103 electron for the Li $2s$ level while 0.240 electron for $2p$ orbitals when Li is adsorbed outside the Z_8 tube. Relaxation of carbon atoms during the adsorption process leads to an increase of the tube C-C distances in the vicinity of the ad-atom. When the C-C bond belonging to the hexagonal adsorption site is parallel to the tube axis, the increase is of 3×10^{-3} nm while it is of 10^{-3} nm when the C-C bond has a strong component along the circumference. Concerning the adsorption energy, its variation is nonmonotonic with the tube radius and we notice that the value for the exo-adsorption (-5.47 eV to -2.40 eV) is always greater than for the endo-adsorption (-3.90 eV to -0.63 eV). This nonmonotonic evolution of the adsorption energy with the tube radius could be due to the complex overlapping evolution of both the $2s$ and $2p$ lithium orbitals with the tube's LUMO lobes. This is confirmed as for atomic hydrogen interaction; our calculation predicts that the adsorption energy smoothly decreases with increasing tube radius.[26] Considering the Z_8 tube, the equilibrium distance between Li and the tube's wall is 0.265 nm when the ad-atom is inside and 0.210 nm when it is outside. This is a general behavior for the zig-zag tubes investigated here, and is directly related to the lower binding energy for the endo-adsorption. The bigger electron transfer from the lithium to the tube in the endo adsorption case reveals a backdonation process from the tube's orbitals to the empty $2p$ states of the ad-atom as this phenomenon is amplified when the equilibrium distance decreases.

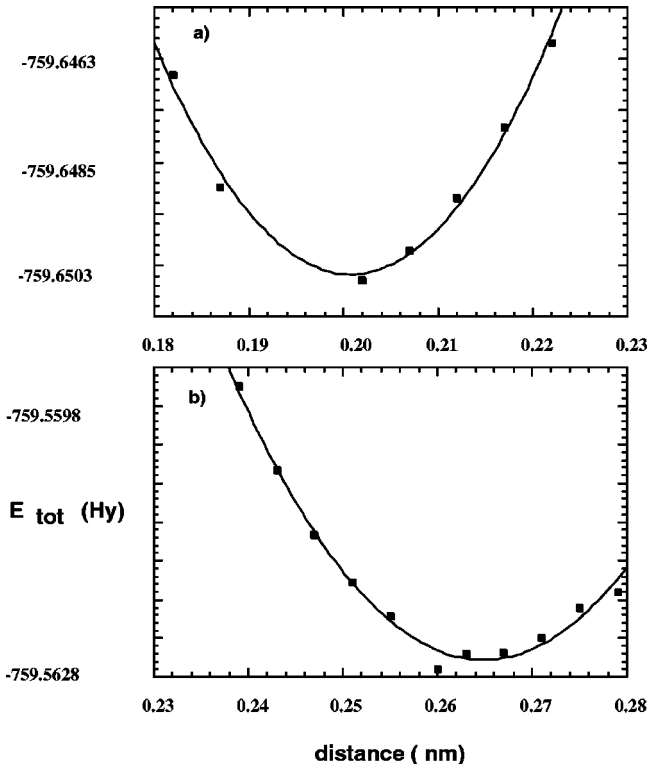

FIG. 4. Total energy of Li adsorbed on a Z_8 nanotube function of the radial Li-tube distance. (a) exo-adsorption; (b) endo-adsorption.

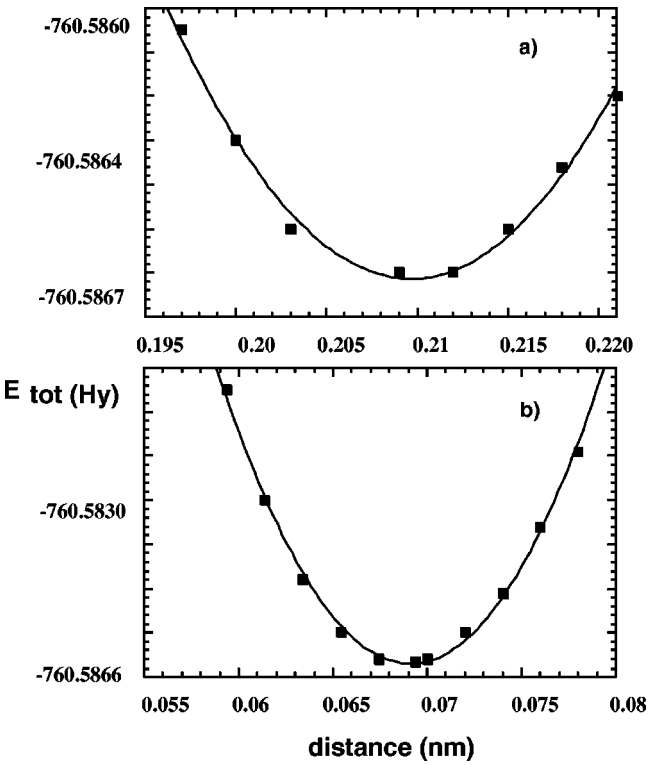

FIG. 5. Total energy of H_2 adsorbed on a Li/Z_8 nanotube. (a) Function of the Li-H_2 distance. (b) function of the H_2 interatomic distance.

From the total energy curves shown in Fig. 4, we can estimate the vibrational frequencies ν corresponding to the radial Li-Z_8 stretching mode. We estimate $\nu=332$ cm^{-1} for the endo-adsorption and $\nu=467$ cm^{-1} for the exo-adsorption, while we calculate $\nu=420$ cm^{-1} for Li adsorbed on a planar graphene molecule. The last computed value is in close agreement with the experimental energy loss obtained by neutron scattering (near $\nu=440$ cm^{-1}) for the [001] L-phonon dispersion in LiC_6 by Zabel.[27] These results confirm the strong influence of the tube curvature on its adsorption property as could be expected from the electronic structure variations with tube shape.[3–6] Simple considerations can be advanced to explain these results by observing the shape of the tube's LUMO depicted in Fig. 3. Equation (1) tells us that the greater the overlapping, the bigger the chemical bonding and thus the adsorption energy. When lithium approaches the tube's surface by the exo-way, the total overlapping will be greater than in the endo way for two reasons: The first is that the tube's LUMO lobes are bigger and away one from each other due to the curvature compared to the graphene case while these lobes are smaller and nearer from each other for the endo-side. The second reason is the sign changes of the LUMO lobes along the circumference. This implies that the overall overlapping of the tube's LUMO and lithium's HOMO is greater on the exo-side than on the endo-side.

When considering the interaction of H_2 with nanotubes,

we found the same behavior as for the graphene case, i.e. the molecule is repealed from the tube's wall both from the endo and the exo-way. On the contrary, when lithium is preadsorbed, our calculation predicts a molecular adsorption of hydrogen at 0.2 nm of the Li ad-atom. The adsorption energy is -0.50 eV when the lithium atom is preadsorbed inside the tube and this value is quite constant with the tube radius. We predict that the molecular complex Li-H_2 is nearly symmetric with an electron transfer of 0.05 electron from each hydrogen atom to Li. The equilibrium geometry obtained for H_2 is 0.0694 nm instead of 0.0680 nm for the free molecule. Such an effect implies a decrease of the H_2 stretching mode for the adsorbed molecule as the H_2 bond decreases under adsorption on the Li center. The total energy (curve b) presented in Fig. 5 allows an estimation of the adsorbed H_2 stretching frequency of $\nu=4078$ cm^{-1} instead of $\nu=4200$ cm^{-1} for the free molecule. The curve (a) corresponds to a Li-H_2 stretching mode characterized by a frequency near $\nu=190$ cm^{-1}. When molecular hydrogen interacts with predsorbed lithium on the exo-side of the tube we also find a stable molecular entity, and a systematic study of the Li-H_2 molecular complex as a function of the tube chirality and radius will be presented elsewhere.[26]

In summary, we found that lithium can be adsorbed inside or outside carbon nanotubes with an adsorption energy depending on the radius of the nanotube and the side of the ad-atom approach. Lithium on carbon nanotube allows the chemisorption of molecular hydrogen. Both adsorbed lithium and Li-H_2 complex should be observable by vibrational spectroscopy. As we have investigated a low coverage limit;'' the effect of the dopant concentration on the surface reactivity should be investigated.

This work was supported by the French CNRS institute. F. Cenedese is specially thanks for is constant help concerning the performance of our team's Mac environnement .

[1] S. Iijima, Nature (London) **354**, 56 (1991).
[2] M.S. Dresselhauss, G. Dresselhauss, and P.C. Eklund, *Science of Fullerenes and Carbon Nanotubes*, (Academic Press, New York, 1995).
[3] J.W. Mintmire, B.I. Dunlap, and C.T. White, Phys. Rev. Lett. **68**, 631 (1992).
[4] N. Hamada, S. Sawada, and A. Oshiyama, Phys. Rev. Lett. **68**, 1579 (1992).
[5] X. Blase, L. Benedict, E.L. Shirley, and S.G. Louie, Phys. Rev. Lett. **72**, 1878 (1994).
[6] J.C. Charlier and Ph. Lambin, Phys. Rev. B **57**, R15 037 (1998).
[7] Proceedings of the Franco-American Conference on Intercalation Compounds of Graphite [Mater Sci. Eng. **31**, (1977)].
[8] G. Gao, T. Cagin, and W.A. Goddard III, Phys. Rev. Lett. **80**, 5556 (1998).
[9] E. Jouguelet, C. Mathis, and P. Petit, Chem. Phys. Lett. **318**, 561 (2000).
[10] R.T. Yang, Carbon **38**, 623 (2000).
[11] P. Chen, X. Wu, J. Lin, and K.L. Tan, Science **285**, 91 (1999).
[12] R.S. Lee, H.J. Kim, J.E. Fisher, J. Lefebvre, M. Radosavljevic, J. Hone, and A.T. Johnson, Phys. Rev. B **61**, 4526 (2000).
[13] A.M. Rao, P.C. Eklund, S. Bandow, A. Thess, and R.E. Smalley, Nature (London) **388**, 257 (1997).
[14] A.C. Dillon, K.M. Jones, T.A. Bekkedahl, C.H. Kiang, D.S. Bethune, and M.J. Heben, Nature (London) **386**, 377 (1997).
[15] G. Stan and M.W. Cole, J. Low Temp. Phys. **110**, 539 (1998).
[16] C.C. Ahn, Y. Ye, B.V. Ratnakumar, C. Witham, R.C. Bowman, Jr., and B. Fultz, Appl. Phys. Lett. **73**, 3378 (1998).
[17] M.J.S. Dewar, E.G. Zoebish, E.F. Healy, and M.J.S. Stewart, J. Am. Chem. Soc. **107**, 3902 (1985).
[18] M.J.S. Stewart, J. Comput. Chem. **10**, 221 (1989).
[19] M.J.S. Stewart and Y.C. Yuan, J. Am. Chem. Soc. **112**, 2088 (1990).
[20] M.J.S. Stewart, J. Am. Chem. Soc. **112**, 2095 (1990).
[21] P.W. Atkins, *Physical Chemistry*, 4th ed. (Oxford University Press, Oxford, 1990).
[22] C.A. Coulson, *Valence* (Oxford University Press, Oxford, 1961).
[23] G. Klopman and R.F. Hudson, Theor. Chim. Acta **9**, 165 (1967).
[24] N.A.W. Holzwarth, S. Rabii, and A. Girifalco, Phys. Rev. B **18**, 5190 (1978).
[25] D.J. Hankinson and J. Almlof, J. Mol. Struct. **388**, 245 (1996).
[26] P. Cenedese and P. Dubot (unpublished).
[27] H. Zabel, A. Magerl, and J.J. Rush, Phys. Rev. B **27**, 3930 (1983).